

Comparative Similarity Analysis of Hypersonic Rarefied Gas Flows Near Simple-Shape Bodies

Vladimir V. Riabov*

Daniel Webster College, Nashua, New Hampshire 03063-1300

Hypersonic viscous flows near simple-shape bodies (wedge, cone, disk, and plate) have been studied numerically under the conditions of wind-tunnel experiments with underexpanded jets. The direct simulation Monte Carlo technique has been used to study the influence of similarity parameters on the flow structure near the bodies and on the aerodynamic coefficients in hypersonic streams of air, nitrogen, helium, and argon. It has been found that, for conditions approaching the hypersonic stabilization limit, the Reynolds number and temperature factor are primary similarity parameters. The influence of other parameters (specific heat ratio, viscosity-approximation parameter, and the Mach number) becomes significant at low Reynolds numbers (less than 10) and small values of the hypersonic similarity parameter (less than 1). The numerical results are in good agreement with experimental data, which were obtained in a vacuum chamber at low and moderate Reynolds numbers from 0.1 to 200. In the studies of the pitching moment and lift coefficients, a three-dimensional numerical approach should be used to simulate nonuniform flow near a plate, cone, and wedge under the experimental conditions with freejets.

Nomenclature

A	= reference area, m ²
C_{m0}	= moment coefficient about the leading edge
C_x	= drag coefficient
C_y	= lift coefficient
CM	= continuum flow
FM	= free molecular flow
h	= plate thickness, m
K	= hypersonic similarity parameter, $M_\infty \sin \theta$
Kn	= Knudsen number
L	= characteristic length, m
M	= Mach number
M_{z0}	= pitching moment about the leading edge, N · m
n	= viscosity-approximation parameter, $\mu \sim T^n$
p	= pressure, N/m ²
Re_0	= Reynolds number, $\rho_\infty V_\infty L / \mu(T_0)$
r	= distance from a nozzle exit along the jet axis, m
T	= temperature, K
t_w	= temperature factor, T_w / T_0
V_∞	= freestream velocity, m/s
x, y	= Cartesian coordinates, m
α	= angle of attack, deg
γ	= ratio of specific heats
δ	= dimensionless plate thickness, h/L
θ	= deflection angle or wedge semiangle, deg
θ_c	= cone semiangle, deg
μ	= viscosity coefficient, N · s/m ²
ρ	= density, kg/m ³
τ	= shear stress, N/m ²

Subscripts

a	= ambient media parameter
CM	= continuum parameter
d	= Mach disk parameter
FM	= free molecular flow parameter
j	= nozzle exit parameter
w	= wall conditions

0	= stagnation flow parameter
∞	= freestream parameter

Introduction

SIMILARITY principles play a fundamental role in applied aerodynamics. In a context of hypersonic viscous flow research, these principles were discussed in reviews by Koppenwallner,¹ Gusev,² Cheng,³ and Anderson.⁴ The free molecular flow regime was also studied by Kogan⁵ and by Muntz.⁶ Similarity criteria for hypersonic flows in the transitional rarefied gas flow regime, which lies between continuum and free molecular flow, were defined by Gusev et al.⁷ Unfortunately, at this time it is impossible to completely simulate high-altitude flight conditions in hypersonic wind tunnels (see notes in Ref. 2). Nevertheless, the technique of partially simulating the major criteria gives valuable information about aerodynamic and thermodynamic characteristics for hypersonic vehicle designers. These studies indicate that the main criterion of similarity is the Reynolds number Re_0 , in which the viscosity coefficient is calculated by means of the stagnation temperature. The influence of other similarity parameters (temperature factor t_w , specific heat ratio γ , viscosity-approximation parameter n , upstream Mach number M_∞ , and hypersonic similarity parameter $K = M_\infty \times \sin \theta$) on aerodynamic characteristics of simple-shape bodies was studied in various experiments.^{8–17}

The Reynolds number Re_0 can be considered as the unique main similarity parameter for modeling hypersonic flows in all three flow regimes: continuum, transitional, and free molecular. Using the Reynolds number Re_0 and other similarity parameters just mentioned, it is possible to construct other well-known parameters.^{1,3,4} For example, in the continuum regime, the Reynolds number Re_0 defines both the interaction parameter^{1,4} χ for pressure approximation and the viscous-interaction parameter^{1,4} V for skin-friction approximation as follows:

$$\chi = \frac{M_\infty^2}{\sqrt{Re_{0,x}}} \sqrt{\frac{2}{\gamma - 1}} \quad (1)$$

$$V = \frac{1}{\sqrt{Re_{0,x}}} \sqrt{\frac{2}{\gamma - 1}} \quad (2)$$

The Reynolds number Re_0 also scales the flow rarefaction, which is characterized by the Knudsen number $Kn_{\infty,L}$ (see Refs. 1, 2, and 7–9) as well as by the viscous-interaction parameter^{1,4} V .

Over the past few decades, significant progress has been made in the numerical simulation of complex rarefied gas flows near simple-shape bodies^{6,7,9,18–26} and about hypersonic vehicles.^{27–30}

Received June 2, 1997; presented as Paper 97-2226 at the AIAA 15th Applied Aerodynamics Conference, Atlanta, GA, June 23–25, 1997; revision received March 23, 1998; accepted for publication April 21, 1998. Copyright © 1998 by the American Institute of Aeronautics and Astronautics, Inc. All rights reserved.

*Adjunct Associate Professor, Department of Engineering, Mathematics and Science, 20 University Drive. Member AIAA.

The generalization of experimental and computational data has resulted in an understanding of the major aero- and thermodynamic characteristics of the bodies and the formulation of the similarity criteria.^{1,2,7,9,31}

In the present study, the influence of similarity parameters Reynolds number Re_0 , t_w , γ , n , Mach number M_∞ , and $K = M_\infty \sin \theta$ on the aerodynamic characteristics (C_x , C_y , and C_{m0}) has been examined. The aerodynamic characteristics of plates, wedges, disks, and sharp cones, as well as the flow structures near the bodies, have been investigated in rarefied flows of helium, argon, nitrogen, and air under test conditions in a vacuum chamber at Knudsen numbers Kn from 0.002 to 7. The numerical results have been obtained by the direct simulation Monte Carlo (DSMC) technique¹⁹ using the DS2G computer code developed by Bird.³² The calculated results have been compared with experimental data that were obtained by Gusev et al.^{8,9} and Riabov.¹²

DSMC Method

The DSMC method has been used in this study as a major numerical simulation technique for low-density gas flows. The basic principles of the technique were described by Bird.^{18,19} The two-dimensional DSMC code³² is used in various parts of the study. Molecular collisions are modeled using the variable hard sphere (VHS) molecular model.³³ The Larsen–Borgnakke statistical model³⁴ is used for modeling the energy exchange between the kinetic and internal modes. The parameters of the VHS molecular model for nitrogen, oxygen, argon, and helium are the same as described by Bird.¹⁹ The gas–surface interactions are assumed to be fully diffuse with full momentum and energy accommodation. Test calculations were previously evaluated for rarefied flows of helium and argon near a sphere and a cylinder.³⁵

In the case of a blunt flat plate, the total number of cells is 1450 in eight zones, the molecules are distributed evenly, and the total number of molecules (from 10,300 to 24,600) corresponds to an average of 7–17 molecules per cell. Following the recommendations of Refs. 18–20, 27, 32, 33, and 36, acceptable results are obtained for an average of at least 10 molecules per cell in the most critical region of the flow. The error is pronounced when this number falls below five, i.e., flow behind the disk. The flow near a wedge is simulated by 11,100–13,500 molecules in 1680 cells of seven zones.

In the case of a disk oriented normally to the upstream flow, a half-space contains 10,200–15,900 molecules located in 800 cells of five zones. The Reynolds number $Re_{0,D}$ varies from 0.1 to 200, and the Knudsen number $Kn_{\infty,D}$ changes from 0.0064 to 7.12 for different gases and flow regimes.

In numerical calculations of the rarefied gas flow near a cone, the recommendations of Bird³⁶ have been used to improve the accuracy of results obtained by the DSMC technique. The total number of cells near a cone (a half-space) is about 18,540, but the molecules are not distributed evenly³⁶ in four zones. An average of at least 10 molecules per cell has been achieved in the area near the axis and the cone surface.

In all cases the usual criterion^{18–20,36} for the time step Δt_m has been realized: $2 \times 10^{-7} \leq \Delta t_m < 1 \times 10^{-6}$ s. Under these conditions, the aerodynamic coefficients become insensitive to the time step.

The location of the external boundary with the upstream flow conditions varies from $0.5L$ (cone, wedge, and plate) to $1.5L$ (disk). Calculations were carried out on a personal computer. The computing time of each variant was estimated to be approximately 20–80 h.

Experiments

The method of strongly underexpanded jets^{7–12} has been used to obtain experimental data over a broad range of the main criterion of similarity, i.e., Reynolds number Re_0 , in which the viscosity coefficient was calculated by means of stagnation temperature T_0 . The value of the Reynolds number Re_0 can be easily changed by relocation of a model along the jet axis at different distances r from a nozzle exit ($Re_0 \sim r^{-2}$).

The structure of viscous gas jets was analyzed by Gusev et al.^{7–11} and Riabov¹² in detail. The main feature of the jet flow is that the flow inside the jet bounded by shock waves becomes significantly overexpanded relative to the outside pressure p_a . The degree of over-

expansion has a maximum value. At sonic conditions in the initial cross section of the jet and at $p_j \gg p_a$, this value is determined by the location of the front shock wave (Mach disk) on the jet axis r_d (Ref. 12):

$$r_d/r_j = 1.34(p_0/p_a)^{\frac{1}{2}} \quad (3)$$

The overexpansion phenomenon is very important for aerodynamic experiments in vacuum wind tunnels. In this case, the restoration of the pressure occurs automatically without the use of a diffuser. The testing was performed in underexpanded viscous jets in a vacuum wind tunnel.

The presence of a nonuniform field in the expanding flow is considered here in terms of the approximation technique of Nikolaev³⁷ and Gusev et al.^{7–11} The relative difference in aerodynamic characteristics in the nonuniform flow from corresponding characteristics in the uniform flow can be evaluated by the parameter L/r , where L is the length of the model and is connected with the presence of axial gradient of density and the difference of the speed vector from the axial direction. The method for the recalculation of aerodynamic characteristics of a wide range of bodies applicable to vacuum wind tunnels was developed by Nikolaev³⁷ and leads to defining some cross section of the flow in which speed and similarity parameters required for the testing should be selected. In this study, the parameters of upstream flow at the point corresponding to the middle of the model were used for the determination of the testing values of aerodynamic coefficients of simple-shape bodies.

The results demonstrated subsequently have been obtained in the strongly underexpanded hypersonic viscous flows, having considered the aforementioned advantages of their applications in aerodynamic experiments. The testing was conducted in the vacuum wind tunnel of the Central Aero-Hydrodynamics Institute (TsAGI, Zhukovsky, Moscow Region, Russia) with different gases: helium, argon, air, and nitrogen at the stagnation temperature $T_0 = 295$ K and at $T_0 = 950$ K. The axisymmetric sonic nozzles with different radii of the critical cross sections r_j were used for obtaining the hypersonic flow. Miniature blunt plates, wedges, disks, and cones were selected as working models ($L \approx 5$ – 12 mm). The coordinate of the front side of the Mach disk r_d was determined by Eq. (3). The influence of viscous and nonequilibrium effects on the density and the flow velocity for all gases was insignificant (see also Ref. 12). Therefore, the main similarity criterion Reynolds number Re_0 and the dynamic pressure were calculated using the nonviscous flow parameters obtained by the method of the characteristics in all processing of the testing data. The errors of the experimental data (6–10%) have been estimated by the techniques described in Refs. 7–12 and 37.

Results

Influence of Mach Number

The study of the influence of Mach number M_∞ on the aerodynamic characteristics of bodies of simple shape has been conducted at small values of Reynolds number and at constant values of other similarity parameters: Re_0 , t_w , γ , and n . The regime of hypersonic stabilization⁴ will occur at $M_\infty \theta \gg 1$ in the case of streamlining of the thin bodies, when the angle θ between the generatrix of the body surface and the direction of the upstream flow becomes small enough. This regime will be realized at smaller values of M_∞ if the angle θ increases.

The dependence of drag and lift coefficients for a wedge ($\theta = 20$ deg) on the angle of attack has been studied in numerical simulations of helium flow at $Re_{0,L} = 4$, $t_w = 1$, and different magnitudes of the freestream Mach number. The results are shown in Figs. 1 and 2 for $M_\infty = 9.9$ (filled circles) and $M_\infty = 11.8$ (filled squares). The base area of the wedge and its length were taken as the reference area and length. The DSMC results indicate a weak dependency of aerodynamic coefficients on Mach number M_∞ in this transitional flow regime. The numerical results correlate well with the experimental data^{9,12} (empty circles and squares), which were obtained in a vacuum wind tunnel at the same flow parameters.

In the free molecular flow regime, the characteristics C_x and C_y (triangles) are not sensitive to changes in upstream flow parameters at $M_\infty \geq 9.9$. Another interesting fact is that the drag coefficient in

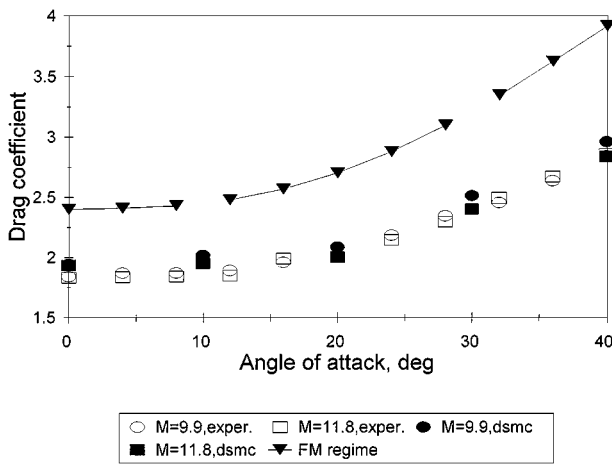


Fig. 1 Drag coefficient C_x for a wedge ($\theta = 20$ deg) at $Re_0 = 4$ and $M_\infty = 9.9$ and 11.8 . Experimental data from Refs. 8, 9, and 12.

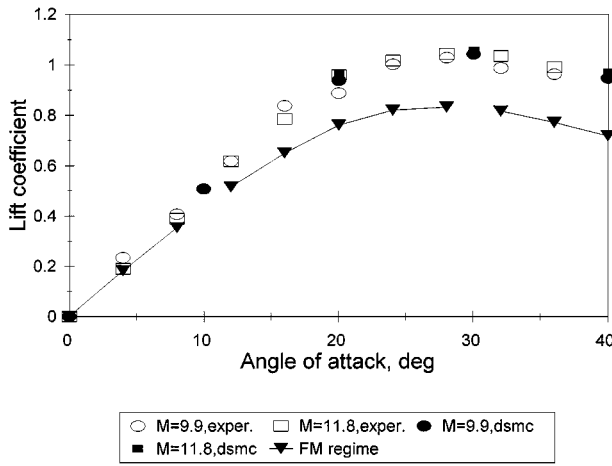


Fig. 2 Lift coefficient C_y for a wedge ($\theta = 20$ deg) at $Re_0 = 4$ and $M_\infty = 9.9$ and 11.8 . Experimental data from Refs. 8, 9, and 12.

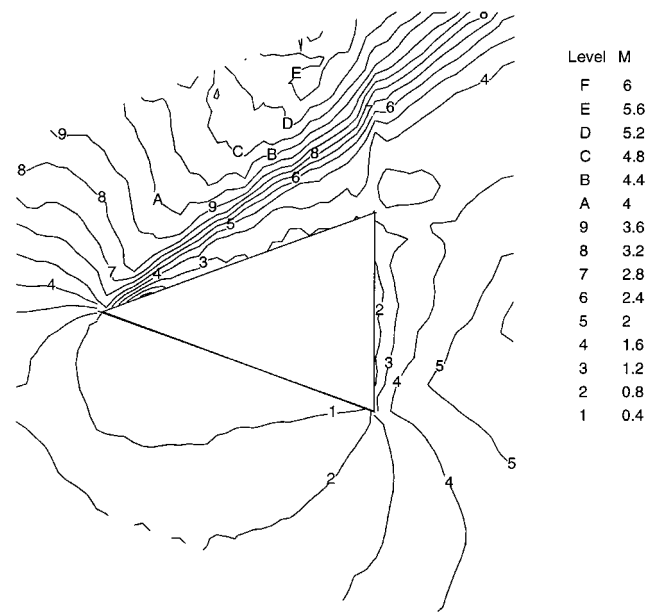


Fig. 4 Mach number contours in helium flow near a wedge ($\theta = 20$ deg) at $Re_0 = 4$, $M_\infty = 11.8$, and $\alpha = 40$ deg.

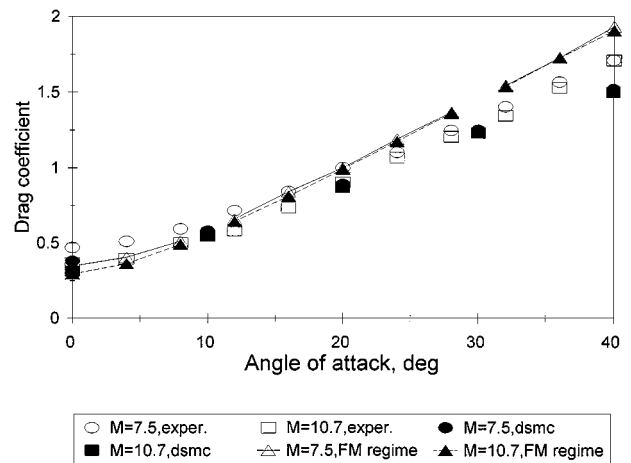


Fig. 5 Drag coefficient C_x for a blunt plate ($\delta = 0.06$) at $Re_0 = 2.46$ and $M_\infty = 7.5$ and 10.7 . Experimental data are from Refs. 8, 9, and 12.

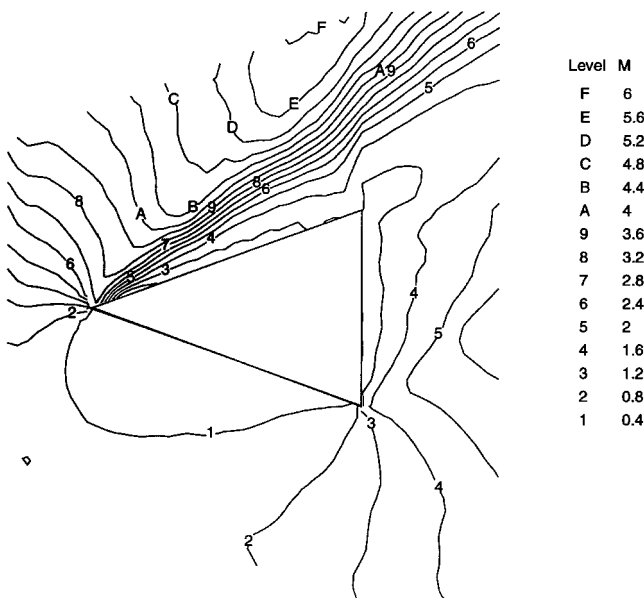


Fig. 3 Mach number contours in helium flow near a wedge ($\theta = 20$ deg) at $Re_0 = 4$, $M_\infty = 9.9$, and $\alpha = 40$ deg.

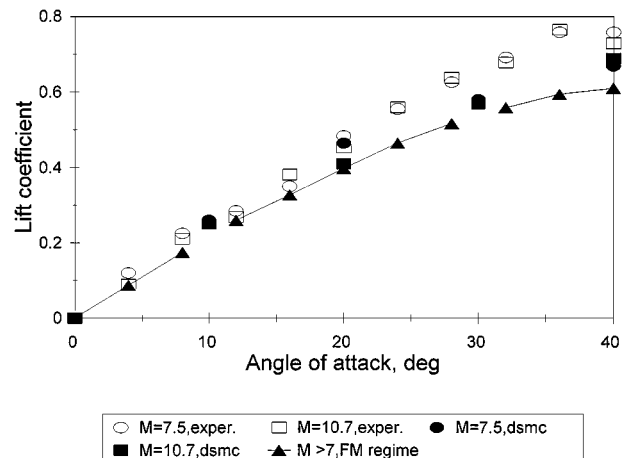


Fig. 6 Lift coefficient C_y for a blunt plate ($\delta = 0.06$) at $Re_0 = 2.46$ and $M_\infty = 7.5$ and 10.7 . Experimental data are from Refs. 8, 9, and 12.

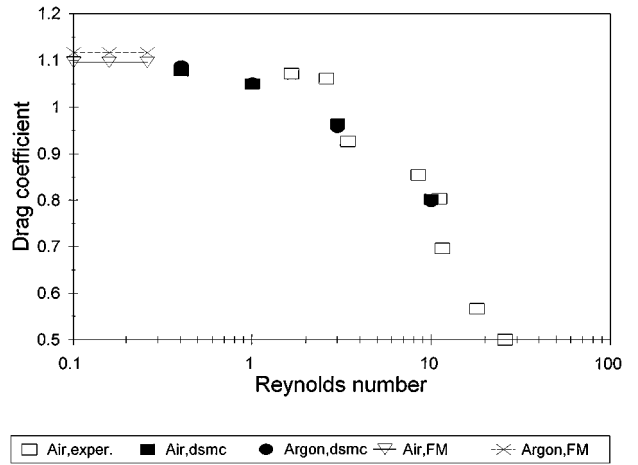
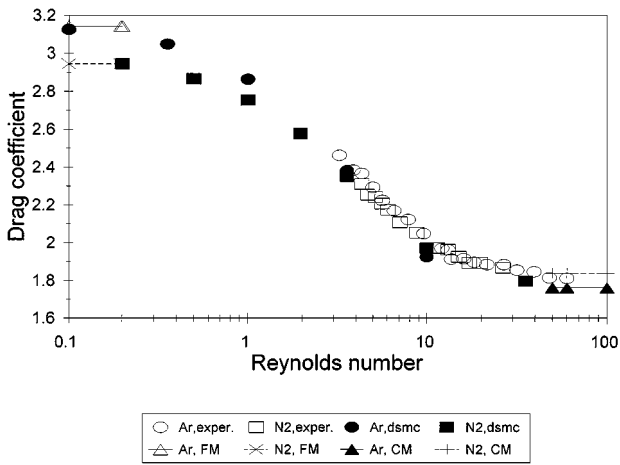


Fig. 7 Drag coefficient C_x for a disk ($\alpha = 90$ deg) vs Reynolds number Re_0 in nitrogen and argon. Experimental data are from Refs. 8 and 9.

Fig. 10 Drag coefficient C_x for a blunt plate ($\delta = 0.1$) vs Reynolds number Re_0 in air and argon at $\alpha = 20$ deg and $t_w = 1$. Experimental data are from Ref. 9.

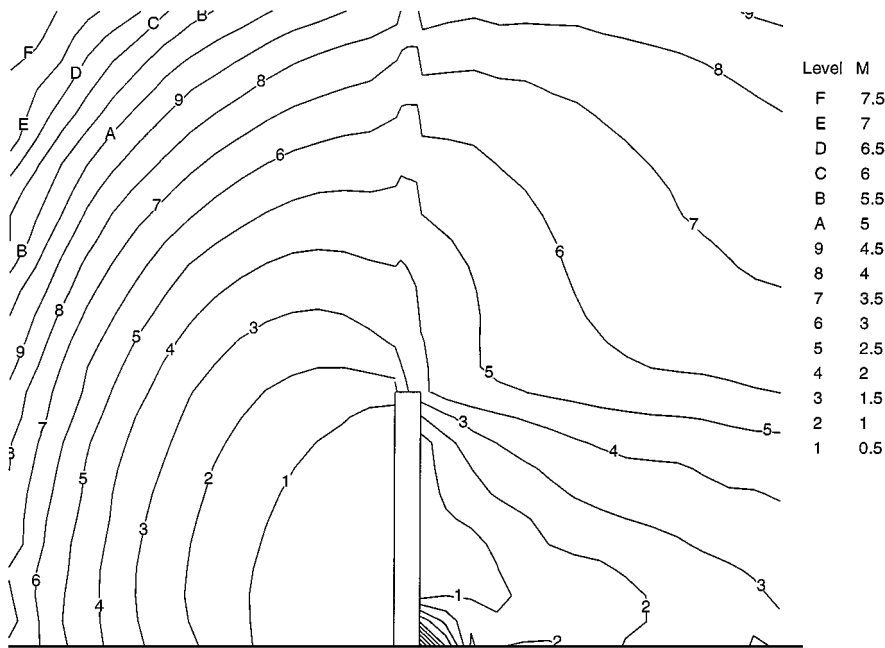


Fig. 8 Mach number contours in nitrogen flow near a disk ($\alpha = 90$ deg) at $Re_0 = 10$, $M_\infty = 10$, and $t_w = 1$.

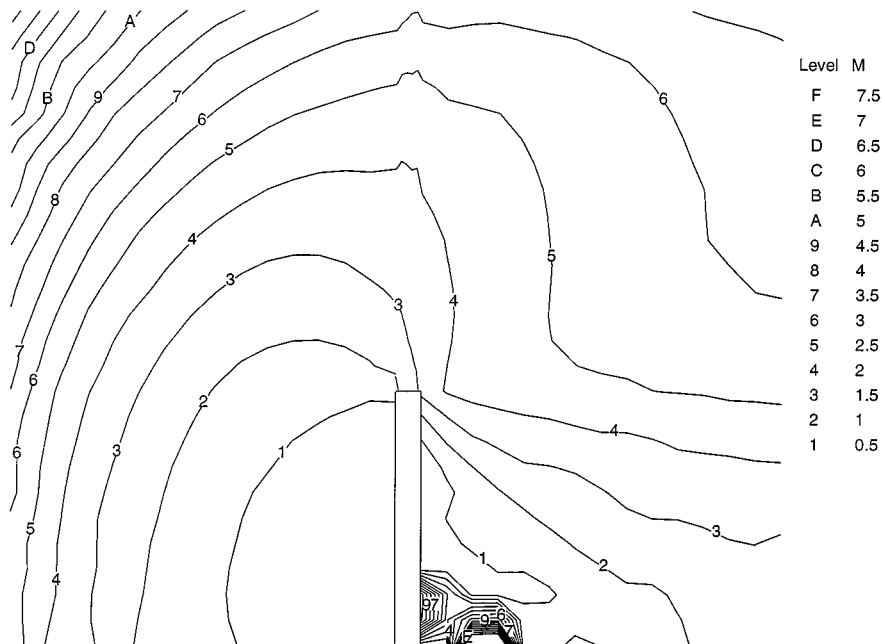


Fig. 9 Mach number contours in argon flow near a disk ($\alpha = 90$ deg) at $Re_0 = 10$, $M_\infty = 10$, and $t_w = 1$.

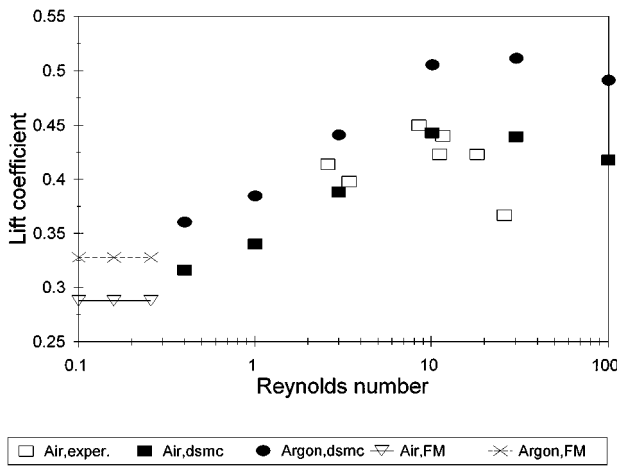


Fig. 11 Lift coefficient C_y for a blunt plate ($\delta = 0.1$) vs Reynolds number Re_0 in air and argon at $\alpha = 20$ deg and $t_w = 1$. Experimental data are from Ref. 9.

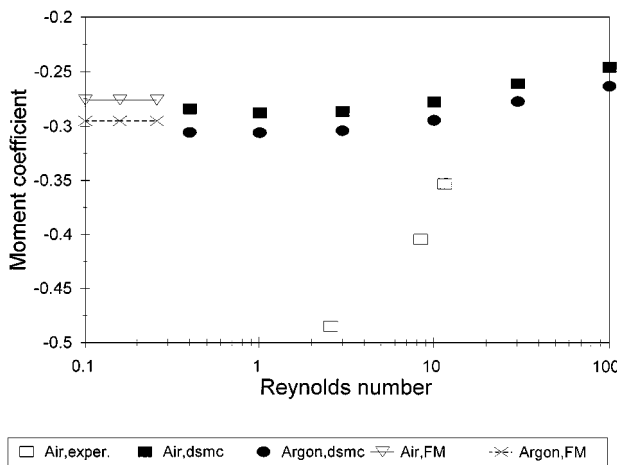


Fig. 12 Pitching moment coefficient C_{m0} about the leading edge for a blunt plate ($\delta = 0.1$) vs the Reynolds number Re_0 in air and argon at $\alpha = 20$ deg and $t_w = 1$. Experimental data are from Ref. 9.

the transitional flow regime is significantly smaller than the free molecular flow coefficient and the lift coefficient is larger by approximately 20% than the corresponding parameter in the free molecular regime (also see Refs. 1, 2, 7, 9, and 12).

The flow pattern near the wedge does not change significantly at different hypersonic upstream flow conditions. The Mach number contours in the flow near the wedge at the angle of attack $\alpha = 40$ deg are given in Figs. 3 and 4 for $M_\infty = 9.9$ and 11.8, respectively.

The results indicate that the hypersonic flow independency principle⁴ is realized in the transitional rarefied flow regime^{9,12} at $K = M_\infty \sin \theta > 1$. As was found in experiments of Gusev et al.^{8,9} and Riabov,¹² this principle is not true for thin bodies at small angles of attack in rarefied gas flows under the conditions $K < 1$.

The drag coefficient of a blunt plate having relative thickness $\delta = h/L = 0.06$ becomes sensitive to the magnitude of the freestream Mach number in helium flow (Fig. 5; $M_\infty = 7.5$ and $M_\infty = 10.7$) at small angles of attack $\alpha \leq 10$ deg. The results calculated by the DSMC technique (filled symbols) correlate well with the experimental data^{8,9,12} (empty symbols). For the lift coefficient, the free molecular flow data, as well as computational and experimental results presented in Fig. 6, are independent of the Mach number, and the value $C_{y,FM}$ is smaller by approximately 15% than the value C_y for transitional flow regime at $\alpha > 16$ deg. This phenomenon was discussed by Gusev et al.^{8,9}

At high angle of attack ($\alpha > 20$ deg), the lift coefficient calculated by the DSMC technique is lower than predicted from the experiment. The difference in the results is because in experiments a three-dimensional slightly nonuniform flow has been studied. The two-dimensional DSMC code has been used to simulate uniform flows in numerical calculations. Nonuniform-flow analysis with a three-dimensional DSMC code should be done in the future.

Influence of the Specific Heat Ratio γ

In the free molecular flow regime, the influence of the specific heat ratio on the aerodynamic characteristics of bodies depends on the normal component of the momentum of the reflected molecules, which is a function of γ . The same phenomenon can be observed at the transitional conditions in the case of the disk at $\alpha = 90$ deg. The nitrogen-argon pair was the most acceptable one for testing.^{8,9,12} The dependencies of C_x of the disk for Ar (filled circles) and N_2 (filled squares) are shown in Fig. 7 for a wide range of Reynolds numbers Re_0 . At the same parameters of the upstream flow, numerical data obtained by the DSMC technique for different models of molecules are compared with experimental data^{8,9} (empty symbols).

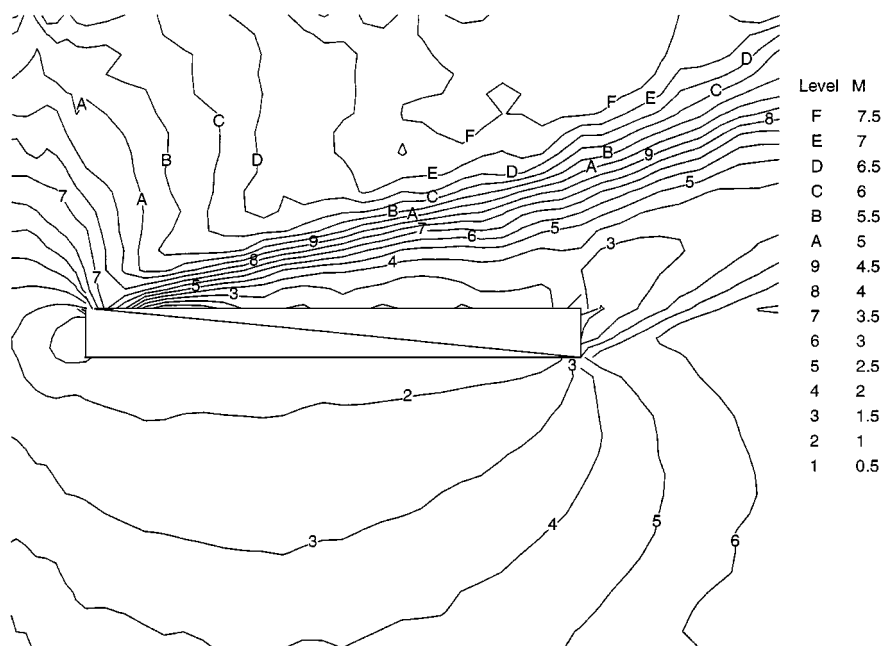


Fig. 13 Mach number contours in airflow near a blunt plate ($\delta = 0.1$) at $\alpha = 20$ deg, $Re_0 = 3$, $M_\infty = 10$, and $t_w = 1$.

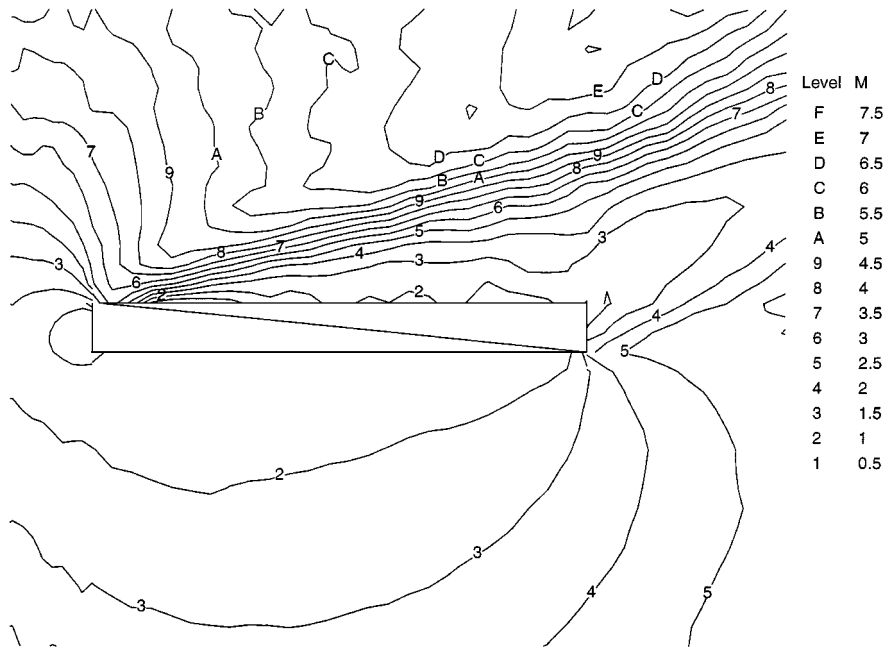


Fig. 14 Mach number contours in argon flow near a blunt plate ($\delta = 0.1$) at $\alpha = 20$ deg, $Re_0 = 3$, $M_\infty = 10$, and $t_w = 1$.

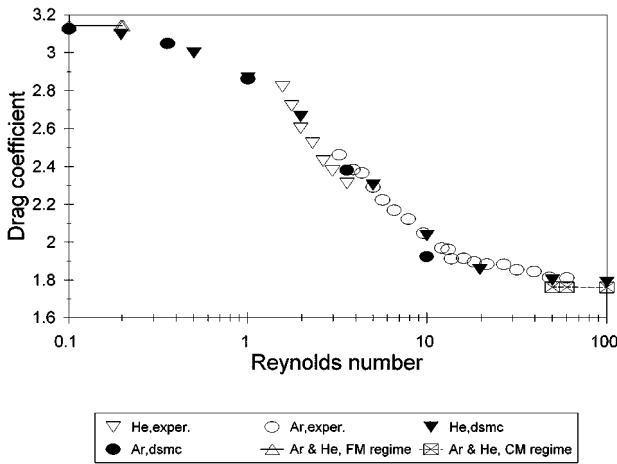


Fig. 15 Drag coefficient C_x for a disk ($\alpha = 90$ deg) vs Reynolds number Re_0 in helium and argon. Experimental data are from Refs. 8 and 9.

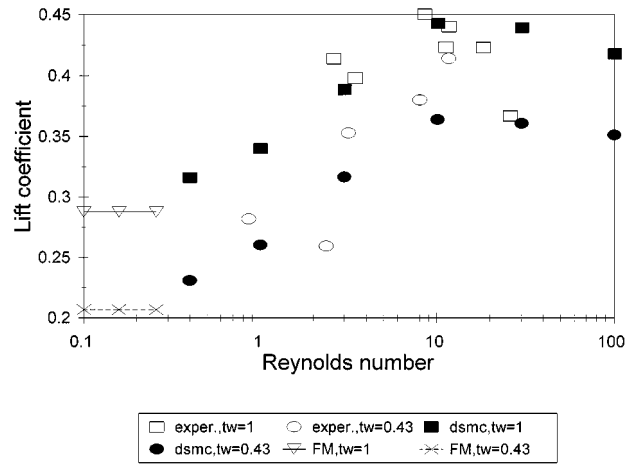


Fig. 17 Lift coefficient C_y for a blunt plate ($\delta = 0.1$) vs Reynolds number Re_0 in air at $\alpha = 20$ deg, $t_w = 1$ and $t_w = 0.43$. Experimental data are from Ref. 9.

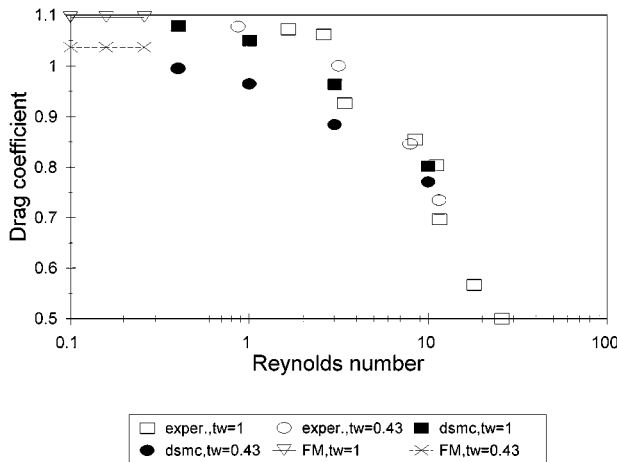


Fig. 16 Drag coefficient C_x for a blunt plate ($\delta = 0.1$) vs Reynolds number Re_0 in air at $\alpha = 20$ deg, $t_w = 1$ and $t_w = 0.43$. Experimental data are from Ref. 9.

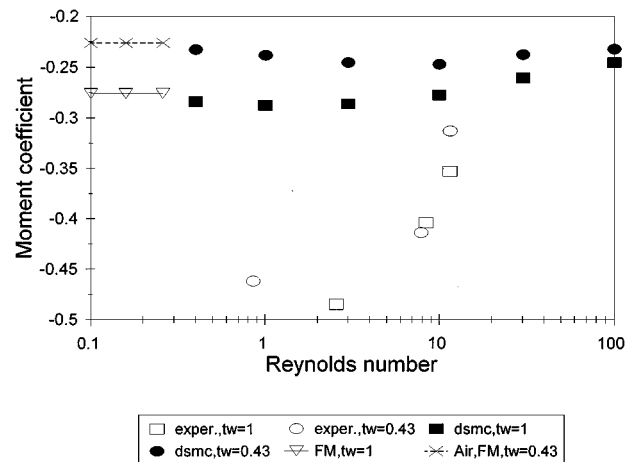


Fig. 18 Pitching moment coefficient C_{m0} about the leading edge for a blunt plate ($\delta = 0.1$) vs Reynolds number Re_0 in air at $\alpha = 20$ deg, $t_w = 1$ and $t_w = 0.43$. Experimental data are from Ref. 9.

The influence of specific heat ratio on the drag coefficient is more significant for small values of $Re_0 < 10$. In the free molecular regime ($Re_0 \rightarrow 0$), an increase in C_x is observed as γ increases.⁵ This increase is caused by the dependence on γ of the reflected momentum of the molecules at $t_w = 1$. The degree of this influence has been evaluated as 8% at $Re_0 < 3$. As the Reynolds number Re_0 increases, this influence decreases, and at $Re_0 > 10$, the drag coefficient of the disk in diatomic gas (nitrogen) becomes larger than that for a monatomic gas. In the continuum flow regime, the dependence of the drag coefficient on the γ difference is insignificant. In this case, at $M_\infty \gg 1$, the drag coefficient of a blunt body can be estimated by a simple Rayleigh formula^{4,9}:

$$C_x = (2/\gamma)[(\gamma + 1)/2]^{2\gamma/(\gamma-1)}[(\gamma + 1)/2\gamma]^{1/(\gamma-1)} \quad (4)$$

The flow structures in diatomic and monatomic gases are essentially different. The Mach number contours obtained from the DSMC results are shown in Figs. 8 and 9 for nitrogen and argon flows, respectively. The subsonic area of the flow is significantly

larger for the monatomic gas. The small irregularities in the Mach contours above the disk can be explained by a grid effect. (The cell size in this area is less by a factor of three than that in the adjacent areas.)

The influence of the specific heat ratio γ on the drag coefficient of thin bodies in the transitional flow regime was studied by Gusev et al.^{8,9} and Riabov¹² for a sharp wedge ($\theta = 20$ deg). This effect was estimated as 4%. In the hypersonic limit⁴ at $M_\infty \gg 1$, the drag coefficient of thin bodies will be proportional to $(\gamma + 1)$.

Detailed analysis of the γ effect for blunt simple-shape bodies has not yet been made. In the present study, the aerodynamic characteristics of a blunt plate ($\delta = 0.1$) are compared for flows in air and argon at $\alpha = 20$ deg, $t_w = 1$, and $0.4 \leq Re_0 \leq 20$ (Figs. 10–12). The specific heat ratio γ insignificantly influences (less than 2%) the drag coefficient of the plate. The major effect of γ is observed in the lift coefficient (Fig. 11) throughout the transitional flow regime. The lift is increased approximately 15% for monatomic gases. As was mentioned earlier, the reflected momentum is significantly dependent on the value of the parameter γ . For example, in the free

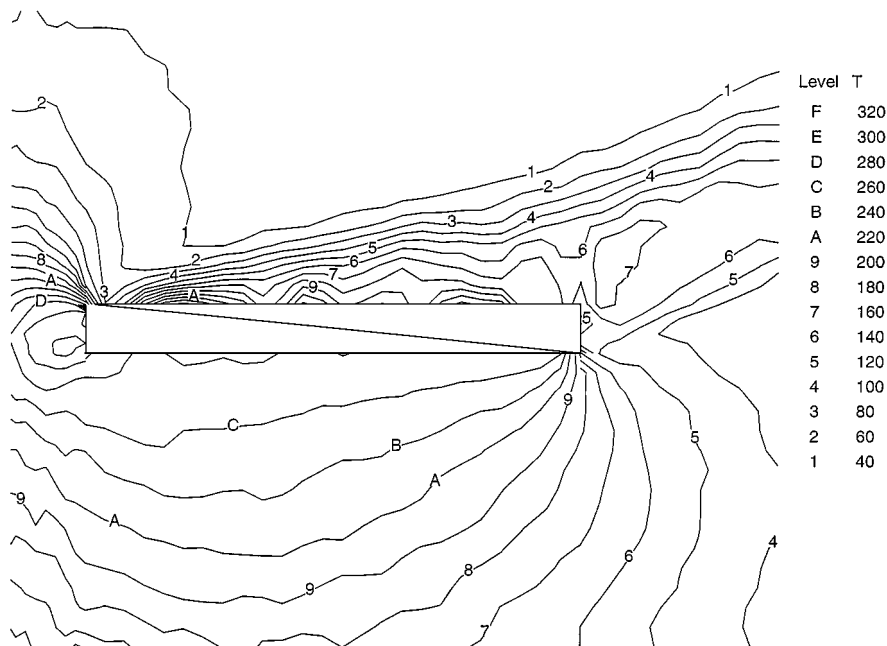


Fig. 19 Temperature contours T , K, in airflow near a blunt plate ($\delta = 0.1$) at $\alpha = 20$ deg, $Re_0 = 3$, $M_\infty = 10$, and $t_w = 1$.

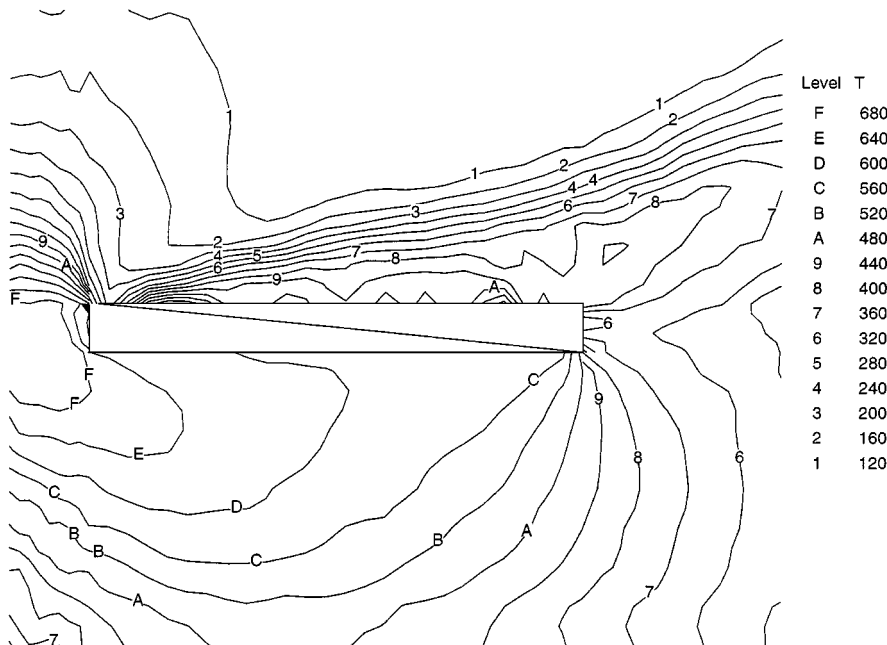


Fig. 20 Temperature contours T , K, in airflow near a blunt plate ($\delta = 0.1$) at $\alpha = 20$ deg, $Re_0 = 3$, $M_\infty = 10$, and $t_w = 0.43$.

molecular flow regime at $K \gg 1$, pressure p_w and shear stress τ can be estimated for a thin body ($\theta \ll 1$) using the following formulas^{5,9}:

$$p_w = 0.5\rho_\infty V_\infty^2 \theta \sqrt{\frac{\Pi(\gamma - 1)}{\gamma} t_w} \quad (5)$$

$$\tau = \rho_\infty V_\infty^2 \theta \quad (6)$$

Analyzing Eqs. (4) and (5), we have to conclude that the parameter γ most influences the lift coefficient. The pitching moment coefficient is also sensitive to changes in the similarity parameter γ but increases by only 6-8% (Fig. 12). Unfortunately, at this time, experimental data for argon are not available.

The accuracy of experimental data in the range $3 \leq Re_0 \leq 30$ has been estimated as 10%. At large values of the Reynolds number, the three-dimensional effects become more significant, and the disagreement between DSMC (two-dimensional code) results and experimental data increases.

The Mach number contours near the plate in the flows of air and argon are shown in Figs. 13 and 14, respectively. In the case of monatomic gas, the sonic zone (a line with $M = 1$) near the plate is displaced farther from the body than for diatomic gas. As a result, pressure and shear stress distributions along the plate become sensitive to the change in the parameter γ .

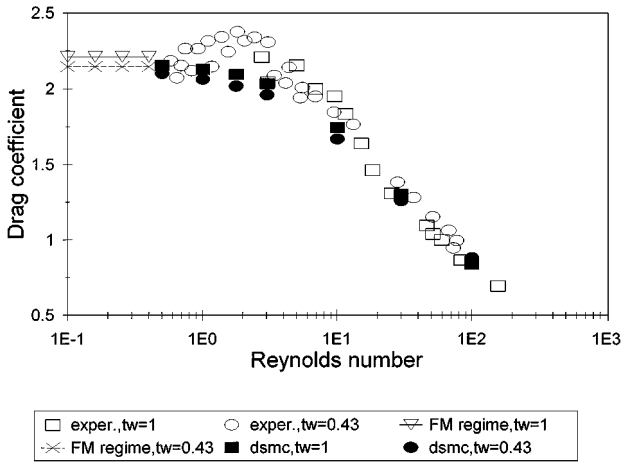


Fig. 21 Drag coefficient C_x for a sharp cone ($\theta_c = 10$ deg) in air at $\alpha = 0$ deg and different temperature factors: $t_w = 1$ and $t_w = 0.43$. Experimental data are from Ref. 9.

Influence of the Viscosity Parameter n

The helium-argon pair is considered for evaluating the influence of the viscosity parameter n , which is used in the approximation of the viscosity coefficient $\mu \sim T^n$. It is noted that the exponent n is closely related to the exponent s in the exponential law of molecular interaction. The exponents n for argon and helium have approximately constant values^{19,38} and differ significantly ($n_{Ar} = 0.87$ and $n_{He} = 0.64$) at $T < 300$ K. The calculation of flow parameters near the disk at $\alpha = 90$ deg (see Fig. 15) was conducted in these gases (filled triangles for He and filled circles for Ar). The experimental data^{8,9} (empty symbols) indicate that an insignificant increase (about 5%) in C_x occurs with the increase in n at $Re_0 < 4$. At the same time, the accuracy of experimental data in the range $1 \leq Re_0 \leq 60$ has been estimated as 8%. In free molecular and continuum flow regimes, this phenomenon is negligible (see the solid and dashed lines, respectively, in Fig. 15).

Influence of the Temperature Factor t_w

Compared to other similarity parameters, the temperature factor ($t_w = T_w/T_0$) is the most important.^{1,2,7-11} As an example, the numerical data for aerodynamic coefficients of a plate ($\delta = 0.06$) are shown in Figs. 16-18 for a wide range of Reynolds number. The lift coefficient (Fig. 17) changes nonmonotonically from the continuum to the free molecular flow regime. Maximum values occur in the transitional flow regime. The influence of the temperature factor can be estimated as 8% for the drag coefficient and as 25% for the lift coefficient. The results correlate well with the experimental data of Gusev et al.^{8,9} except for the pitching moment coefficient. In the transitional flow regime this coefficient becomes more sensitive to the accommodation coefficients, which have been considered as full accommodation with diffuse reflection in the DSMC calculations. In the calculation, a two-dimensional approach has been employed, which is not accurate to predict the pressure and shear stress distributions on the model as well as the pitching moment. Detailed analysis of this discrepancy in aerodynamic characteristics will be studied in future research.

Temperature contours in the airflow near a blunt plate at $M_\infty = 10$, $Re_0 = 3$, and $\alpha = 20$ deg are shown in Figs. 19 and 20 at values for the temperature factor t_w of 1 and 0.43, respectively. The structure of the temperature fields in front of the plate is significantly different in these cases. In the case of the cold wall at $t_w = 0.43$, a significant temperature-jump effect takes place along the surface (Fig. 20). As a result, local temperature parameters (or factors), pressure, and shear stress are significantly different at different locations on the body surface. Decreasing the temperature factor significantly decreases the pressure at the body surface in comparison

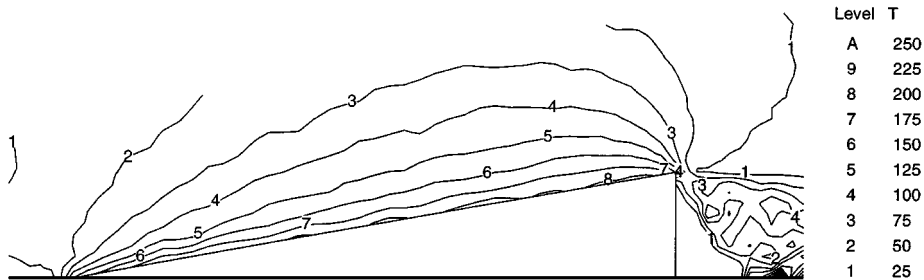


Fig. 22 Temperature contours T , K, in airflow near a sharp cone ($\theta_c = 10$ deg) at $\alpha = 0$ deg, $Re_0 = 3$, $M_\infty = 10$, and $t_w = 1$.

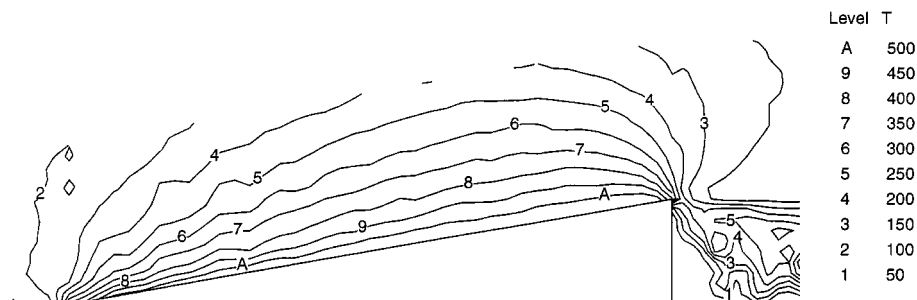


Fig. 23 Temperature contours T , K, in airflow near a sharp cone ($\theta_c = 10$ deg) at $\alpha = 0$ deg, $Re_0 = 3$, $M_\infty = 10$, and $t_w = 0.43$.

with the tangential stresses⁹ [also see Eqs. (5) and (6)]. Therefore, the lift coefficient is the most sensitive aerodynamic parameter to changes in t_w in the transitional and free molecular flow regimes (see Fig. 17). A similar effect of the nonmonotonical dependency of the lift coefficient on Reynolds number was found in the case of a sharp cone.^{7,9}

The temperature factor effect on the drag coefficient of a thin body has been studied numerically for a sharp cone with semiangle $\theta_c = 10$ deg at $\alpha = 0$ deg in air (Fig. 21). It was found that, at $t_w = 0.43$ and $Re_0 \leq 30$, the drag coefficient is 5–10% lower compared with that for a hot wall ($t_w = 1$). The numerical data are compared with the experimental data of Gusev et al.⁹ Both sets of data correlate well at $Re_0 \leq 0.8$ and > 10 . The maximum value of the drag coefficient at $Re_0 \sim 3$ and $t_w = 0.43$ has not been found in calculations. One of the reasons for this difference is the nonuniform flow conditions in experiments with underexpanded jets.^{7,9,12} At small values of the cone semiangle $\theta_c \leq 10$ deg and nonuniform flow conditions, the use of the average Reynolds number Re_0 can generate additional errors related to approximation procedures. Also the average temperature of the cone surface ($T_w = 450$ K) has been used in an interpretation of experimental data. In fact, the temperature was not constant along the surface of the cone. In the past, several attempts were unsuccessfully made to avoid this problem in the case of the miniature models of a cone by using a liquid-nitrogen cooler. Only the constant-temperature approach has been realized by the DSMC technique. The gas-surface interactions are assumed to be fully diffuse with full momentum and energy accommodation in the calculations. This approach does not exactly correspond to the actual experimental conditions.

The temperature contours in airflow near a sharp cone at $t_w = 1$ and $t_w = 0.43$ are shown in Figs. 22 and 23, respectively. The cloud of hot gas occupies a larger area near the body for $t_w = 0.34$ than for $t_w = 1$. Analysis of the influence of these phenomena on the normal and tangential stresses is an area for future research.

Summary

New information about hypersonic viscous rarefied gas flows near simple-shape bodies has been obtained and can be effectively used for investigation and prediction of aerothermodynamic characteristics of hypersonic vehicles during the design of their missions in complex rarefied atmospheric conditions of the Earth and other planets. Fundamental insight into the characteristics and similarity parameters of these flows was obtained. For conditions approaching the hypersonic limit, the Reynolds number Re_0 and temperature factor t_w are the primary similarity parameters. The influence of other parameters (the specific heat ratio γ , viscosity parameter n , and Mach number M_∞) is significant at $M_\infty \theta \ll 1$ and $Re_0 < 10$. The abnormal increase in the pitching momentum coefficient for the blunt plate and the drag coefficient of the sharp cone at low Reynolds numbers should be verified in future experiments and numerical calculations based on three-dimensional nonuniform flow analysis.

Acknowledgments

The author would like to express gratitude to G. A. Bird for the opportunity to use the DS2G computer program and to V. N. Gusev, A. I. Erofeev, T. V. Klimova, and V. A. Perepukhov for their fruitful participation in developing methods for solution of the problem.

References

- Koppenwallner, G., "Fundamentals of Hypersonics: Aerodynamics and Heat Transfer," *Hypersonic Aerothermodynamics*, Deutsche Forschungs- und Versuchsanstalt für Luft- und Raumfahrt E.V., Lecture Series, No. 1984-01, DFVLR Press, Göttingen, Germany, 1984, pp. 1–56.
- Gusev, V. N., "High-Altitude Aerothermodynamics," *Fluid Dynamics*, Vol. 28, No. 2, 1993, pp. 269–276.
- Cheng, H. K., "Perspectives on Hypersonic Viscous Flow Research," *Annual Review of Fluid Mechanics*, Vol. 25, 1993, pp. 455–484.
- Anderson, J. D., Jr., *Hypersonic and High Temperature Gas Dynamics*, McGraw-Hill, New York, 1989, pp. 213–332.
- Kogan, M. N., *Rarefied Gas Dynamics*, Academic, New York, 1969, Chap. 6.
- Muntz, E. P., "Rarefied Gas Dynamics," *Annual Review of Fluid Mechanics*, Vol. 21, 1989, pp. 387–417.

⁷Gusev, V. N., Kogan, M. N., and Perepukhov, V. A., "The Similarity and Aerodynamic Measurements in Transitional Regime at Hypersonic Velocities," *Uchenyye Zapiski TsAGI*, Vol. 1, No. 1, 1970, pp. 24–31 (in Russian).

⁸Gusev, V. N., Klimova, T. V., and Riabov, V. V., "The Main Regularities of Aerodynamic Characteristics Changes in the Transitional Regimes of Hypersonic Flows," *Uchenyye Zapiski TsAGI*, Vol. 7, No. 3, 1976, pp. 47–57 (in Russian).

⁹Gusev, V. N., Erofeev, A. I., Klimova, T. V., Perepukhov, V. A., Riabov, V. V., and Tolstykh, A. I., "Theoretical and Experimental Investigations of Flow over Simple Shape Bodies by a Hypersonic Stream of Rarefied Gas," *Trudy TsAGI*, No. 1855, 1977, pp. 3–43 (in Russian).

¹⁰Gusev, V. N., Klimova, T. V., and Lipin, A. V., "Aerodynamic Characteristics of the Bodies in the Transitional Regime of Hypersonic Flows," *Trudy TsAGI*, No. 1411, 1972, pp. 3–53 (in Russian).

¹¹Gusev, V. N., Nikol'skii, Yu. V., and Chernikova, L. G., "Heat Transfer and Hypersonic Rarefied Gas Flow Streamlining of the Bodies," *Heat and Mass Transfer (Minsk)*, Vol. 1, May 1972, pp. 254–262 (in Russian).

¹²Riabov, V. V., "Aerodynamic Applications of Underexpanded Hypersonic Viscous Jets," *Journal of Aircraft*, Vol. 32, No. 3, 1995, pp. 471–479.

¹³Kienappel, K., Koppenwallner, G., and Legge, H., "Force and Heat Transfer Measurements on Inclined Cones in the Hypersonic Range from Continuum to Free Molecular Flow," *Proceedings of the 8th International Symposium on Rarefied Gas Dynamics*, Academic, New York, 1974, pp. 317–325.

¹⁴Legge, H., "Force and Heat Transfer Measurements in Hypersonic Free-Jet Flow," AIAA Paper 94-2633, June 1994.

¹⁵Keel, A. G., Jr., Chamberlain, T. E., and Willis, D. R., "Near-Free Molecular Disk Drag: Theory and Experiment," *Proceedings of the 8th International Symposium on Rarefied Gas Dynamics*, Academic, New York, 1974, pp. 327–333.

¹⁶Dahlen, G. A., and Brundin, C. L., "Wall Temperature Effects on Rarefied Hypersonic Cone Drag," *Proceedings of the 13th International Symposium on Rarefied Gas Dynamics*, Vol. 1, Plenum, New York, 1985, pp. 453–460.

¹⁷Lengrand, J. C., Allège, J., Chpoun, A., and Raffin, M., "Rarefied Hypersonic Flow over a Sharp Flat Plate: Numerical and Experimental Results," *Rarefied Gas Dynamics: Space Science and Engineering*, Vol. 160, Progress in Astronautics and Aeronautics, AIAA, Washington, DC, 1994, pp. 276–284.

¹⁸Bird, G. A., *Molecular Gas Dynamics*, Oxford Univ. Press, Oxford, England, UK, 1976, Chap. 9.

¹⁹Bird, G. A., *Molecular Gas Dynamics and the Direct Simulation of Gas Flows*, Oxford Univ. Press, Oxford, England, UK, 1994, pp. 334–377.

²⁰Bird, G. A., "Monte Carlo Simulation of Gas Flows," *Annual Review of Fluid Mechanics*, Vol. 10, 1978, pp. 11–31.

²¹Yen, S. M., "Numerical Solution of the Nonlinear Boltzmann Equation for Nonequilibrium Gas Flow Problems," *Annual Review of Fluid Mechanics*, Vol. 16, 1984, pp. 67–97.

²²Erofeev, A. I., and Perepukhov, V. A., "The Calculation of Streamlining of the Endless Plate in Rarefied Gas Flow," *Uchenyye Zapiski TsAGI*, Vol. 7, No. 1, 1976, pp. 102–106 (in Russian).

²³Erofeev, A. I., and Perepukhov, V. A., "Hypersonic Rarefied Flow About a Flat Plate by the Direct Simulation Method," *Proceedings of the 11th International Symposium on Rarefied Gas Dynamics*, Vol. 1, Commissariat a L'Energie Atomique, Paris, France, 1979, pp. 417–426.

²⁴Gorelov, S. L., and Erofeev, A. I., "Qualitative Features of a Rarefied Gas Flow About Simple Shape Bodies," *Proceedings of the 13th International Symposium on Rarefied Gas Dynamics*, Vol. 1, Plenum, New York, 1985, pp. 515–521.

²⁵Belotserkovskii, O. M., Erofeev, A. I., and Yanitskii, V. E., "Direct Monte-Carlo Simulation of Aerohydrodynamic Problems," *Proceedings of the 13th International Symposium on Rarefied Gas Dynamics*, Vol. 1, Plenum, New York, 1985, pp. 313–332.

²⁶Lu, Y., Gottesdiener, L., and Lengrand, J.-C., "Direct Simulation Monte Carlo Calculation of Sphere Drag in Low Supersonic Transition Flows," *Rarefied Gas Dynamics: Theory and Simulations*, Vol. 159, Progress in Astronautics and Aeronautics, AIAA, Washington, DC, 1994, pp. 294–302.

²⁷Bird, G. A., "Application of the Direct Simulation Monte Carlo Method to the Full Shuttle Geometry," AIAA Paper 90-1692, June 1990.

²⁸Rault, D., "Efficient Three-Dimensional Direct Simulation Monte Carlo for Complex Geometry Problems," *Rarefied Gas Dynamics: Theory and Simulations*, Vol. 159, Progress in Astronautics and Aeronautics, AIAA, Washington, DC, 1994, pp. 137–154.

²⁹Ivanov, M. S., Antonov, S. G., Gimelshein, S. F., and Kashkovsky, A. V., "Computational Tools for Rarefied Aerodynamics," *Rarefied Gas Dynamics: Space Science and Engineering*, Vol. 160, Progress in Astronautics and Aeronautics, AIAA, Washington, DC, 1994, pp. 115–126.

³⁰Moss, J. N., Rault, D. F. G., and Price, J. M., "Direct Monte Carlo Simulations of Hypersonic Viscous Interactions Including Separations,"

Rarefied Gas Dynamics: Space Science and Engineering, Vol. 160, Progress in Astronautics and Aeronautics, AIAA, Washington, DC, 1994, pp. 199–208.

³¹Gusev, V. N., Erofeev, A. I., Provotorov, V. P., and Yegorov, I. V., “Numerical Simulation and Experiment in Rarefied Gas Dynamics,” *Proceedings of the 20th International Symposium on Rarefied Gas Dynamics*, Inst. of Mechanics, Chinese Academy of Sciences, Beijing, PRC, 1996, p. E1.

³²Bird, G. A., “The DS2G Program User’s Guide, Version 1.0,” G.A.B. Consulting Pty Ltd., Killara, New South Wales, Australia, Jan. 1995, pp. 1–50.

³³Bird, G. A., “Monte-Carlo Simulation in an Engineering Context,” *Rarefied Gas Dynamics*, edited by S. S. Fisher, Vol. 74, Progress in Astronautics and Aeronautics, AIAA, New York, 1981, pp. 239–255.

³⁴Borgnakke, C., and Larsen, P. S., “Statistical Collision Model for Monte

Carlo Simulation of Polyatomic Gas Mixture,” *Journal of Computational Physics*, Vol. 18, No. 4, 1975, pp. 405–420.

³⁵Riabov, V. V., “Numerical Analysis of Compression and Expansion Binary Gas-Mixture Flows,” AIAA Paper 96-0109, Jan. 1996.

³⁶Bird, G. A., “Rarefied Hypersonic Flow Past a Slender Sharp Cone,” *Proceedings of the 13th International Symposium on Rarefied Gas Dynamics*, Vol. 1, Plenum, New York, 1985, pp. 349–356.

³⁷Nikolaev, V. S., “Aerodynamic and Thermal Characteristics of Simple Shape Bodies in a Nonuniform Flow,” *Trudy TsAGI*, No. 1709, 1975, pp. 3–25 (in Russian).

³⁸Vargaftik, I. B., *Handbook of the Thermophysical Properties of Gases and Liquids*, Nauka, Moscow, 1972, pp. 191–225 (in Russian).

R. G. Wilmoth
Associate Editor